OPTIMAL GROUPING FOR A NUCLEAR MAGNETIC RESONANCE (NMR) SCANNER*

NICO VANDAELE
UFSIA, University of Antwerp, Belgium
nico.vandaele@ua.ac.be

INNEKE VAN NIEUWENHUYSE
Research Assistant of the Fund for Scientific Research-Flanders (Belgium)
UFSIA, University of Antwerp, Belgium
inneke.vannieuwenhuyse@ua.ac.be

SASCHA CUPERS
UFSIA, University of Antwerp, Belgium

ABSTRACT

In this paper we analyze how a Nuclear Magnetic Resonance Scanner can be managed more efficiently, simultaneously improving patient comfort (in terms of total time spent in the system) and increasing availability in case of emergency calls. By means of a superposition approach, all relevant data on the arrival and service process of different patient types are transformed into a general single server, single class queueing model. The objective function consists of the weighted average patient lead time, which is a multi-dimensional convex function of the different patient group sizes. The "optimal" patient group sizes are determined by means of a dedicated optimization routine. The model does not only provide a valuable aid for planning purposes, but also allows to model customer service. It is illustrated by means of real life data, obtained from the Virga Jesse Hospital (Hasselt, Belgium).

* This research was supported by the BOF fund of the University of Antwerp-UFSIA.

Keywords: Queueing, Health Services, Performance Analysis, Lot Sizing

1. INTRODUCTION

Modern technology plays a vital role in today's hospital infrastructure, both in the field of the medical sciences and within the area of hospital management. On the one hand, the use of high tech equipment is necessary in order to provide high quality health care. On the other hand, this quality level has to be obtained by operating the hospital's scarce and expensive resources in the most efficient way, without endangering availability and responsiveness.

The Nuclear Magnetic Resonance scanner (named NMR hereafter) is one of these very expensive high tech resources, used for medical imaging. In this paper we will analyze how the use of this resource can be managed in a more efficient way, by controlling the group sizes of different patient types in such a way that the weighted average patient lead time is minimized. As will be shown, this does not only improve patient comfort (in terms of total time spent in the system), but also the responsiveness of the system (in terms of availability in case of emergency calls).

The analysis is done by means of a mathematical model ([1],[2]), which is applied to real-life data from the NMR department Virga Jesse hospital in Hasselt (Belgium). To obtain insight in this medical imaging technique, we first discuss the operational characteristics of the NMR. Next, we develop the mathematical model which will be used to address the group size decision problem. In a third section the results of the case study are discussed. Finally, a last section summarizes the most important conclusions.

2. OPERATIONAL CHARACTERISTICS OF THE NMR

The NMR technology is based on three subsequent steps: nuclear magnetization, resonance and relaxation.

- **Nuclear magnetization:**

The nuclei of the atoms of the human body have a particular property, called spin, resembling a self-rotation of the nucleus. When these nuclei enter a strong magnetic field, they execute a so-called precession spin having a specific frequency (the *precession frequency*). Due to the external magnetic field, most nuclei put themselves into a stable orientation, which means that only a small amount of energy is needed to keep the nuclei in this position.

- **Resonance:**
  The stable situation is disturbed by adding a particular amount of external energy to the system. This additional energy is produced by a radio frequency source, of which the frequency equals the precession frequency (hence the term *resonance*).
- **Relaxation:**
  In the final stage, the external energy source is removed and the system returns to its stable situation. During this process, the system releases electromagnetic energy, which is registered by a sensitive antenna and afterwards transformed into electric signals. Finally, a computer processes the electrical intensities and the image can be constructed.

The NMR equipment consists of a strong electromagnet and a set of measuring antennas. The electromagnet is cylindrical, allowing the accommodation of the appropriate part of the human body. At the central point of the cylinder, the magnetic field is the most homogeneous.

The antennas are specifically developed in function of the part of the human body to be measured. As a consequence, each time another type of image is needed, the system has to switch to the appropriate antenna or the antenna has to be set up differently. In either case, a combination of both hardware and software setups has to be performed [3].

Because of these setups, the grouping of patients is a common practice in medical imaging departments. Although the need for grouping is quite obvious, determining the optimal size of the groups is not self-evident. On the one hand there is a need to use the NMR equipment efficiently, which means that the number of setups must be kept low and group sizes should be large.

On the other hand, patients cannot wait too long before being processed, as patient lead time has become an important element of competition between hospitals. This argument speaks in favor of small group sizes.

In order to explain this inherent conflict, we analyze the relationship between the average patient lead time (defined as the time between a patient's call arrival at the NMR department and the moment at which he leaves the system) and the group size. This relationship is represented in Figure 1.

The two conflicting effects mentioned above are referred to as the *grouping effect* and the *saturation effect* [4]. The grouping effect (straight line on Figure 1) shows increasing average patient lead times when groups are larger. The larger the group, the longer the group lead time, and subsequently the longer the patients will remain in the system. The saturation effect (dotted line on Figure 1) shows increasing lead times when groups are smaller. Smaller groups require more frequent setups, and as a consequence, the utilization of the NMR equipment increases. This causes congestion, resulting in longer average lead times.

The combination of both effects results in a convex relationship [4], which implies that there is an optimal group size minimizing average patient lead time. More details can be found in [1].

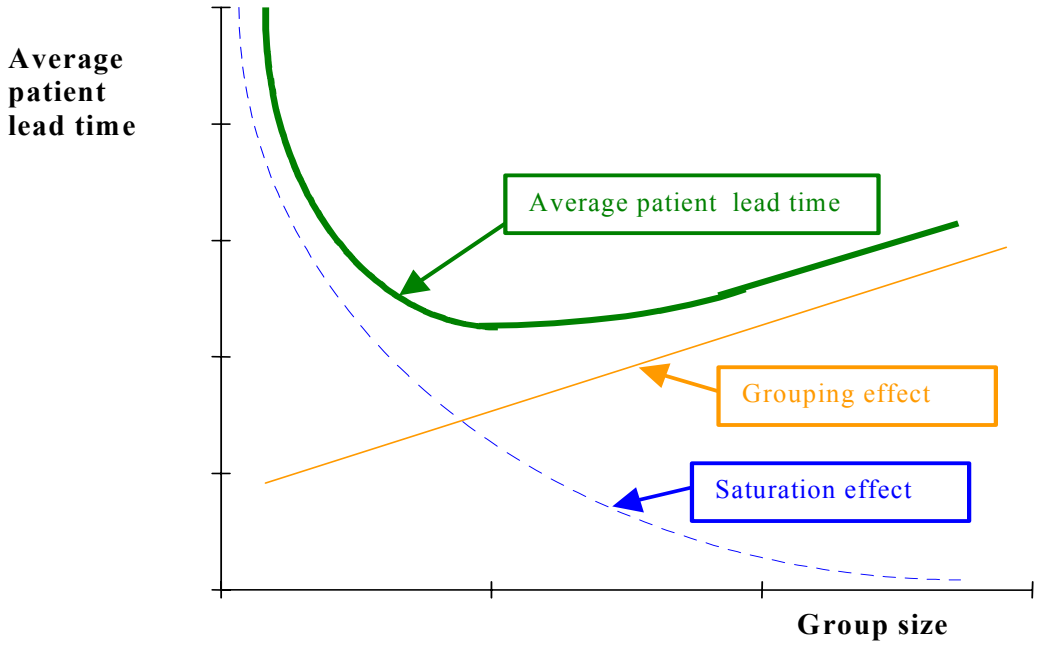

Figure 1: Convex relationship between average patient lead time and group size

In the following paragraph, we develop the mathematical model we will use to address the group size decision problem. The objective is to determine the group size that minimizes the average patient lead time. Clearly, this is not only desirable from a patient's point of view (since it improves patient comfort), but also enhances the responsiveness of the system.

3. MODEL DEVELOPMENT

General setting

In our approach, the NMR is regarded as a multi-product, single server open queueing model. As such, it is an extension of the single product, single server model described in [6]. If we view a request for a particular image (part of the human body) as an arrival of that image type, we can define the parameters of the model as follows:

- k image type index, *1, …, K*
- Y_k average interarrival time of image type k
- s^2_{Yk} interarrival time variance of image type k

- c^2_{Yk} squared coefficient of variation of the interarrival time of image type *k*
- λ_k average arrival rate of image type *k*

  $= \frac{1}{\overline{Y}_k}$
- $\overline{T}_k$ average setup time for image type *k*
- s^2_{Tk} setup time variance for image type *k*
- c^2_{Tk} squared coefficient of variation of the setup time of image type *k*
- $\overline{X}_k$ average unit processing time of image type *k*
- s^2_{Xk} unit processing time variance for image type *k*
- c^2_{Xk} squared coefficient of the unit processing time of image type *k*
- μ_k unit processing rate of image type *k*

  $= \frac{1}{\overline{X}_k}$

Throughout the analysis, it is assumed that each patient going through the scanner requires only one particular image type to be taken. In order to construct the model, the parameters of the individual arrival and service processes are aggregated into a single aggregate arrival and service process. Simultaneously, we integrate the grouping aspect of the service process into our model.

The aggregate arrival process

Assuming a processing group size of Q_k for image type k, the average time between two successive arrivals of such a processing group is equal to $Q_k Y_k$. The average group arrival rate of image type *k* is then given by l_k:

$$l_k = \frac{\lambda_k}{Q_k} \qquad (1)$$

The aggregate group arrival rate at the scanner can be calculated by summing up the group arrival rates of the different image types:

$$l = \sum_{k=1}^{K} l_k \qquad (2)$$

The squared coefficient of variation of the group interarrival time for image type *k* can be calculated as follows:

$$ca_k^2 = \frac{c_{Yk}^2}{Q_k} \qquad (3)$$

The squared coefficient of variation of the aggregate group interarrival time at the scanner is approximated by

$$ca^2 \approx \frac{1}{3} + \frac{2}{3}\left(\sum_{k=1}^{K} \frac{l_k}{l} ca_k^2\right) \qquad \textit{for K > 1}$$

(4)

The first term of this formula is constant, the second term represents a weighted average of the squared coefficients of variation of the individual group interarrival times. Further details on this approximation can be found in [1] and [2].

At this point the aggregate arrival process is modeled. We now turn to the aggregate group service process.

The aggregate group service process

The average aggregate group processing time is calculated as a weighted average of the individual group processing times:

$$\frac{1}{\mu} = \sum_{k=1}^{K} \frac{l_k}{l}\left[\overline{T}_k + Q_k \overline{X}_k\right] \qquad (5)$$

The weights reflect the relative importance of the group arrivals of the different image types.

The squared coefficient of the aggregate group processing times equals

$$cs^2 = \left[\sum_{k=1}^{K} \frac{l_k}{l}\left[\overline{T}_k + Q_k \overline{X}_k\right]^2\right]\mu^2 - 1 + \sum_{k=1}^{K} \frac{l_k}{l} \frac{\left[s_{Tk}^2 + Q_k s_{Xk}^2\right]}{\left[\overline{T}_k + Q_k \overline{X}_k\right]^2} \qquad (6)$$

and can be split up in two variability effects. The first part of the equation reflects the differences in average group processing times among the image types. As such, it can be seen as a measure of *heterogeneity between the image types*: if all average setup and processing times are equal, the first part becomes zero.

The last term is a weighted average of the squared coefficients of variation of the individual group processing times. As such, it can be seen as a measure of the *variability inherent in the processing times of the individual image types*. If all setup and processing times are deterministic, this sum equals zero. Note that all aggregate arrival and processing characteristics are functions of the group size Q_k.

Given the aggregate arrival rate l and the aggregate processing rate μ, we can now calculate the effective traffic intensity ρ_e. It is a measure of the load of the scanner, and can be derived from the traditional traffic intensity ρ by adding the effect from the setup times [7]:

$$\rho_e = \frac{l}{\mu} = \sum_{k=1}^{K} l_k \left[\overline{T}_k + Q_k \overline{X}_k \right] = \sum_{k=1}^{K} l_k \overline{T}_k + \rho \qquad (7)$$

where ρ is defined as

$$\rho = \sum_{k=1}^{K} \rho_k = \sum_{k=1}^{K} \frac{\lambda_k}{\mu_k} \qquad (8)$$

From equation (7) it is clear that the effective traffic intensity is dependent on the group sizes Q_k. For large group sizes l_k tends to zero, and ρ_e approaches the traditional traffic intensity ρ. For small group sizes, ρ_e increases due to the impact of the setup times.

Note that in order to preserve system stability, ρ_e should strictly be smaller than unity. This constraint implies that there is a lower bound on the group sizes that can be used in the system. Note however that the individual lower bounds per image type are highly interdependent so that it is only possible to state a uniform lower bound for the entire set of image types.

Objective function and optimization

Given the average group arrival rate λ_k and average group processing rate μ_k, the expected lead time for each image type k can be obtained:

$$E(W_k) = \frac{Q_k - 1}{2\lambda_k} + E(W_q) + \overline{T}_k + \frac{Q_k + 1}{2\mu_k} \qquad (9)$$

This lead time clearly consists of four building blocks. The first term corresponds to the average time a patient of image type k will have to wait until a group of size Q_k has been formed (*collection time*). The term $E(W_q)$

stands for the average time that patients spend waiting in queue in front of the scanner until it becomes idle (*waiting time*). The last two terms correspond to the average time a patient of image type *k* spends in setup and processing.

These different phases are visualized in Figure 2, for a group size of four patients. The model assumes a FIFO-discipline, which is accepted to be fair among patients in a waiting room.

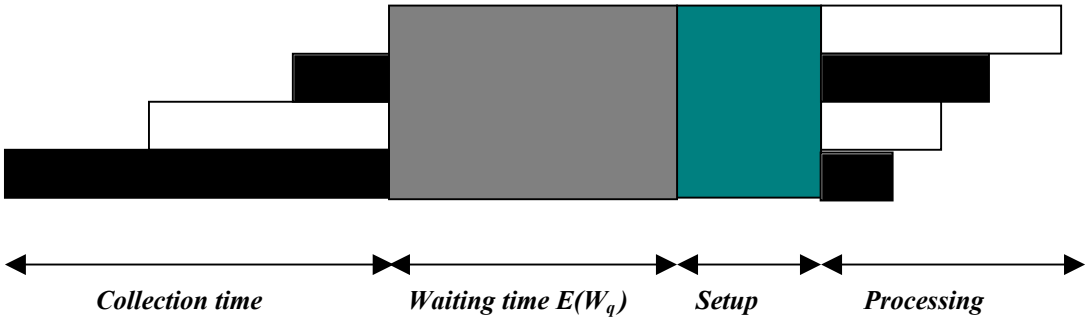

Figure 2: Visualization of the different phases of the group lead time

As can be seen from the figure, the collection time is different for each patient of the group: the first patient has to wait until the other three have arrived, while after arrival of the last patient the entire group is immediately transferred to the second stage namely the queue in front of the scanner. The time spent in queue and setup is the same for each patient of the group. The time spent in processing is again different: given the FIFO-discipline and the fact that the scanner can deal with only one patient at a time, the first patient will be processed immediately while the others will have to wait until the preceding patient has left the system.

The expected waiting time $E(W_q)$ is approximated by the Kraemer-Lagenbach Belz formula [8], and is independent of the image type:

$$E(W_q) = \frac{\rho_e^{\,2}\left(ca^2 + cs^2\right)}{2l\left(1-\rho_e\right)} \exp\left\{\frac{-2\left(1-\rho_e\right)\left(1-ca^2\right)^2}{3\rho_e\left(ca^2+cs^2\right)}\right\} \quad \text{if} \quad ca^2 \le 1$$

$$E(W_q) = \frac{\rho_e^{\,2}\left(ca^2 + cs^2\right)}{2l\left(1-\rho_e\right)} \quad \text{if} \quad ca^2 \ge 1 \qquad (10)$$

Finally, the aggregate average lead time $E(W)$ is calculated as a weighted average of the lead times of all individual image types:

$$E(W) = E(W_q) + \sum_{k=1}^{K} \frac{\lambda_k}{\sum_{k=1}^{K} \lambda_k} \left[\frac{Q_k - 1}{2\lambda_k} + \overline{T}_k + \frac{Q_k - 1}{2\mu_k} \right] \tag{11}$$

The weights are chosen to reflect the relative importance of each image type for the system. Here, the importance is measured by means of the volume of the image type. Alternatively, other weighting factors could be applied.

At this point the model is completed and we can formally state our optimization problem:

$$\textbf{Min} \qquad E(W) = E(W_q) + \sum_{k=1}^{K} \frac{\lambda_k}{\sum_{k=1}^{K} \lambda_k} \left[\frac{Q_k - 1}{2\lambda_k} + \overline{T}_k + \frac{Q_k + 1}{2\mu_k} \right]$$

$$\textbf{s.t.} \qquad \rho_e < 1$$

$$Q_k \geq 1$$

This non-linear constrained optimization problem is solved using a dedicated optimization algorithm, yielding the optimal group size Q_k^* for each image type *k* [1].

The expected individual lead time for a patient of image type *k* can then be obtained by entering Q_k^* into Equation (9):

$$E(W_k)_{OPT} = \frac{Q_k^* - 1}{2\lambda_k} + E(W_q)(Q_k^*) + \overline{T}_k + \frac{Q_k^* + 1}{2\mu_k} \tag{12}$$

The variance of this optimal individual lead time is given by:

$$V(W_k) = \frac{Q_k^* - 1}{2} s_{Yk}^2 + \frac{(Q_k^* - 1)(Q_k^* + 1)}{12\lambda_k^2} + V(W_q) + s_{Tk}^2 + \frac{Q_k^* + 1}{2} s_{Xk}^2$$

$$+ \frac{(Q_k^* + 1)(Q_k^* - 1)}{12\mu_k^2} - \frac{(Q_k^* - 1)(Q_k^* + 1)}{6\lambda_k \mu_k} \tag{13}$$

In this formula, $V(W_q)$ stands for the variance of the waiting time spent in queue and is not dependent on the product type. It is approximated using the formula of Whitt [9].

Assuming a lognormal distribution for the individual patient lead times, the values of $E(W_k)$ and $V(W_k)$ enable us to calculate the minimal lead time W_{Pk} that the hospital has to quote to the patients in order to guarantee a certain customer service level P_k[1]:

$$W_{Pk} = \exp\{\beta_k + z_{Pk}\gamma_k\}$$

with $$\beta_k = \ln\left(\frac{E(W_k)}{\sqrt{\frac{V(W_k)}{E(W_k)^2}+1}}\right)$$

$$\gamma_k^2 = \ln\left(\frac{V(W_k)}{E(W_k)^2}+1\right)$$

The difference between W_{Pk} and $E(W_k)$ is referred to as *safety time*.

[1] The customer service level P_k is defined as the percentage of time that patients of type k are served within the quoted lead time

4. APPLICATION: THE NMR DEPARTMENT AT THE VIRGA JESSE HOSPITAL (HASSELT, BELGIUM)

General setting

The Virga Jesse Hospital is a medium-sized hospital located in Hasselt (Belgium). In 1998, it had a capacity of 567 beds, and employed about 1500 people among which some 130 physicians. About 18,000 patients were treated and the hospital reached a total of 175,000 patient-days. The hospital has a modern medical imaging department, including an NMR scanner where the model described above was put into practice.

Each day, the NMR scanner is staffed by one radiologist and two administrators. The radiologist operates the NMR and dictates the medical reports (protocols). The administrators keep track of the appointments, write reports, print out the images, take care of the preliminary treatment of the patients and perform the setups.

The NMR scanner produces ten types of images, only five of which occur frequently. In Table 1 those five image types are described (Image type 1 to 5). The infrequent image types are summarized in Image type 6.

Image type #	***Name***	***Abbreviation***
1	Skull/Foot/Ankle	SFA
2	Lumbal spine	LS
3	Cervical spine	CS
4	Shoulder/Hip	SH
5	Knee/Wrist/Elbow	KWE
6	Rest (neck, breast, etc.)	REST

Table 1: Overview of the six image types for the NMR scanner

The scanner is available five days a week, from 7h55 to 18h55, minus a 1 hour break used for cleaning. On Tuesday, the NMR is only available as from

8h10 due to a meeting. So in total the scanner is available 10 hours a day, except on Tuesday (9.45 hours). Patients are registered between 8h00 and 19h00, including noon. In our study there is no distinction between internal patients (coming from another hospital department) and external patients (coming from outside).

Description of the arrival and service process

The NMR scanning operation itself consists of four phases:

- **Setup:** one setup is performed for each group of patients
- **Preparation:** time to prepare the patient including moving, covering specific parts of the body, etc.
- **Operation time:** time needed to carry out the measurements and process the calculations
- **Post-operation time:** time needed to leave the NMR scanner.

The time needed to carry out the measurements is dependent on the image type (ranging from 12 seconds to 7 minutes) and the number of measurements (ranging from 3 to 8). A rule of thumb is that the smaller the part of the human body, the more measurements have to be performed. The patient also influences the number of measurements: nervousness or movements can cause the measurement to be redone, increasing processing variability.

The NMR scanner was observed during several weeks in order to collect the necessary data. The arrival data (for individual patients) are summarized in Table 2.

Image type	Average interarrival time (seconds) (minutes)		Variance of the interarrival time (seconds²)	SCV of the interarrival time	Average arrival rate (# patients/sec)
1	14400	(240)	288376200	1.391	0.0000694
2	6120	(102)	25416000	0.679	0.0001634
3	7971.43		144803314	2.279	0.0001254

	(132.86)				
4	27390	(456.5)	353248200	0.471	0.0000365
5	5375	(89.58)	16207500	0.561	0.0001860
6	17850	(297.5)	477405000	1.498	0.0000560

Table 2: Summary of the arrival data for the different image types

As can be seen, there are significant differences in the frequencies of occurrence for the individual image types. In addition, the image types seem to exhibit a significantly different variability.

The observed setup time and processing time characteristics are given in Table 3 and Table 4.

Image type	Average setup time (seconds)	Setup time variance (seconds²)	Setup time SCV
1	46.714	338.905	0.155
2	89.375	1745.982	0.219
3	77.857	882.143	0.146
4	80	3200	0.500
5	91	2318.667	0.280
6	110	7725	0.638

Table 3: Summary of the setup time data for the different image types

Image type	Average processing time (seconds) (minutes)		Processing time variance (seconds²)	Processing time SCV
1	1525	(25.416)	244445.45	0.105
2	1163.571	(19.39)	113157.143	0.0836
3	1102.5	(18.375)	64740	0.0533

4	1428	(23.8)	34920	0.017
5	947.59	(15.79)	53840.39	0.06
6	1640	(27.33)	37200	0.0138

Table 4: Summary of the processing time data for the different image types

For all product types, the average setup and processing times are in the same order of magnitude. The processing times exhibit significantly less variability than the setup times.

It is important to recall that the time scale on which the arrivals are registered does not coincide with the time the NMR scanner is available for processing. As already mentioned, patients are registered between 8h00 and 19h00 (including noon). The time that the scanner itself is available differs due to time losses such as the possible late arrival of the radiologist, noon breaks, or smaller time losses due to various reasons. To put the arrival and service time data on the same scale, we introduce the availability factor A, defined as

$$A = \frac{m_f}{m_f + m_r}$$

where m_f equals the mean uptime and m_r equals the mean downtime. During the period of our observations, the lunch break lasted for an average of 6495 seconds, while the radiologist was absent 600 seconds on average. This means that the scanner was unavailable for service during 7095 seconds on average (m_r) on a total of 39600 seconds ($m_r + m_f$), leading to an availability A of 82 %.

The corresponding average and variance of the effective setup time then become [7]:

$$\overline{T}'_k = \frac{\overline{T}_k}{A}$$

$$s'^2_{Tk} = \frac{s^2_{Tk}}{A^2}$$

For the average and variance of the effective processing time we get

$$\overline{X}'_k = \frac{\overline{X}_k}{A}$$

$$s'^2_{Xk} = \frac{s^2_{Xk}}{A^2}$$

respectively. We use these expressions as conservative approximations, as we can learn from [7]. Table 5 shows the effective setup and processing time data for the NMR.

Image type	Effective average setup time (seconds)	Effective setup time variance (seconds²)	Effective average processing time (seconds)	Effective processing time variance (seconds²)
1	56.910	503.000	1857.868	362803.935
2	108.883	2591.372	1417.548	167946.905
3	94.851	1309.2769	1343.147	96086.578
4	97.462	4749.414	1739.695	51827.978
5	110.863	3441.347	1154.424	79909.466
6	134.010	11465.382	1997.970	55211.935

Table 5: Effective setup and processing time data

At this point we have all the necessary data to run the optimization model. The results are discussed in the next section.

Optimization: results

The resulting optimal group sizes (rounded above (+) and rounded below (-)) are shown in Table 6, along with the planned group sizes and the actual group sizes as currently used in practice.

Image Type	Planned group sizes		Actual group sizes		Optimal group sizes	
	(+)	(-)	(+)	(-)	(+)	(-)
Overall	8	7	3	2	NA NA	
1	8	7	2	1	2	1
2	6	6	4	3	2	1
3	7	7	2	2	3	2
4	5	5	3	2	2	1
5	13	12	5	4	2	1
6	5	5	1	1	2	1

Table 6: Optimal group sizes versus planned and actual group sizes

The planned group sizes are the group sizes used by the administration to list incoming calls/arrivals whereas the actual group sizes represent the registered practice. In this way the actual and the planned group sizes represent the group sizes with and without the unplanned emergency calls.

Given the convex relationship from Figure 1, rounding to the nearest larger integer is a conservative approach. On the contrary, rounding the nearest lower integer is opportunistic but can in certain situations lead to infeasibilities (due to the effect of the increased time spent on setups, which may lead to an adapted traffic intensity equal to or larger than unity).

The table shows a significant difference between the planned group sizes and the actual group sizes. The reasons for this are diverse: emergencies, patient related causes (e.g. late arrivals, cancellations), wrong diagnosis by the corresponding physician, etc. As the resulting actual group sizes are always smaller than the planned group sizes, the actual number of setups performed is larger than planned. Furthermore, Table 6 shows that the optimal group sizes (as calculated by the model) confirm the actual batch sizes, and even indicate opportunities for further group size reduction for image types 2, 4 and 5.

Table 7 gives an overview of the respective average patient lead times, as well as the improvement (in terms of percentage) in average patient lead time that could be obtained by using the optimal group sizes instead of the actual group sizes. We can conclude that group sizes of 2 would be optimal, except for type 3 which needs a group size of 3 (these optimal group sizes are all rounded to the larger integer, as rounding to the smaller integer leads to infeasibilities). As can be seen, the lead time improvements range between ca 5 % for type 6 patients up to 48 % for type 5 patients. As such, it is clear that using these optimal group sizes would enhance patient comfort and in the meantime improve the availability of the NMR in case of emergency operations. Since the group sizes used in practice are mainly a management decision, it can be concluded that the model provides hospital management with powerful and yet easy to implement guidelines for efficiency improvement.

Image Type	Planned group size	**Planned LT sec (min)**	Actual group size	**Actual LT sec (min)**	Optimal group size	**Optimal LT sec (min)**
1	8	100268.17 (1671.14)	2	45219.17 (753.65)	2	32380.57 (539.68)
			% lead time improvement = 29 %			
2	6	58862.49 (981.04)	4	49205.60 (820.09)	2	27411.90 (456.86)
			% lead time improvement = 44 %			
3	7	68359.49 (1139.32)	2	41013.39 (683.56)	3	33503.64 (558.39)
			% lead time improvement = 19 %			
4	5	98524.26 (1642.01)	3	66953.07 (1115.88)	2	38679.77 (644.66)
			% lead time improvement = 42 %			

5	13	82319.69 (1371.94)	5	50879.51 (847.99)	2	26515.13 (441.92)
			% lead time improvement = 48 %			
6	5	80772.18 (1346.20)	1	36378.51 (606.31)	2	34462.87 (574.38)
			% lead time improvement = 5 %			

Table 7: Average patient lead times in seconds (minutes) for the planned, the actual and the optimal group sizes, all rounded to the largest smaller integer

In order to ensure a desired service level P_k for each image type k, the hospital will have to include *safety time* in the lead time it quotes to its patients. This safety time is primarily reflected in the so-called *backlog* (i.e. the time between the receipt of the call for an appointment and the date of the appointment). Assuming a lognormal distribution for the patient lead time, the model enables us to calculate the minimal lead time needed to ensure a certain service level P_k for image type k. Table 8 gives the results for different service levels.

Image Type	Average Lead Time	Standard Dev. Lead Time	Lead time service level 80 %	90 %	95 %	99 %
1	1.00 (3.09)	0.82 (1.83)	1.42 (4.23)	1.93 (5.38)	2.51 (6.56)	4.09 (9.55)
2	0.84 (1.81)	0.71 (1.24)	1.20 (2.53)	1.65 (3.31)	2.15 (4.15)	3.54 (6.33)
3	1.03 (2.11)	0.81 (1.42)	1.46 (2.93)	1.98 (3.83)	2.54 (4.78)	4.08 (7.28)
4	1.19 (3.03)	0.91 (1.86)	1.68 (4.17)	2.26 (5.34)	2.88 (6.55)	4.58 (9.65)
5	0.82 (2.53)	0.70 (1.36)	1.16 (3.42)	1.61 (4.26)	2.11 (5.11)	3.50 (7.21)

6	1.06	0.88	1.51	2.07	2.69	4.42
	(2.49)	(1.70)	(3.47)	(4.55)	(5.68)	(8.67)

Table 8: Average, standard deviation and percentiles of the patient's lead times in days for the planned and the optimal batch sizes.

The data in bold correspond to the optimal group sizes, the data between brackets to the planned group sizes, which coincide with the current appointment practice. All data are expressed in working days. The 99% percentile for the planned batch sizes confirms the current backlog of about two weeks. By using the optimal group sizes, this backlog could be cut roughly by half.

A similar safety time rationale can be applied to the actual time spent in the NMR department at the day of the appointment. This time is hereafter referred to as *operational lead time*, and includes waiting time in queue, setup time and processing time. Table 9 gives an overview of the observed average and variance of this operational lead time for each image type *k*, expressed in seconds (minutes). From this table it is clear that the average operational lead time is dependent on the image type, ranging from 36 minutes for type 2 up to 57 minutes for type 4.

Image Type	**Average operational lead time (seconds) (minutes)**		**Variance operational lead time (seconds²)**
1	3040	(50.67)	1643127.273
2	2142.857	(35.71)	523161.905
3	2385	(39.75)	1691280
4	3432	(57.2)	3877920
5	2201.379	(36.69)	736998.0296
6	2820	(47)	111600

Table 9: Average and variance of the observed operational lead times

Image type	Average Waiting Time (minutes)	Standard Dev. Waiting Time (minutes)	Waiting time service level			
			80 %	90 %	95 %	99 %
1	25.84	10.90	33.54	40.03	46.33	61.10
2	18.21	6.15	22.79	26.31	29.62	37.09
3	20.27	11.05	27.42	34.26	41.19	58.38
4	29.17	16.74	39.75	50.19	60.86	87.66
5	18.71	7.30	23.98	28.26	32.38	41.88
6	23.97	2.84	26.31	27.70	28.91	31.34

Table 10: Average, standard deviation and percentiles of a patient's operational waiting time in minutes

If a schedule of appointments is put forward, the patient should be present some time before the appointment. This time can be seen as a percentile of the operational waiting time (operational lead time excluding setup and processing time), for a certain confidence level.

Table 10 gives an overview of the average[2], standard deviation and percentiles of the operational waiting time for different confidence levels. This table reveals that the average and variance of the operational waiting time depend on the image type, which is also reflected in the operational waiting time percentiles. For example, to make sure that the proposed schedule can be met with 95% probability, a patient of type 1 should be present at the NMR department 46.33 minutes before the time his/her appointment is scheduled; a patient of type 4 however should be present 60.86 minutes in advance.

5. CONCLUSION

[2] On average, 51 % of the operational lead time is spent waiting.

In this paper we showed that the operational aspects of a NMR scanner can be approximated by using a queueing model. As each different image type requires a setup time, patients of the same image type should be grouped together. The queueing model enables the user to calculate the optimal group size for each image type *k*, minimizing the weighted average lead time and thus increasing patient comfort and improving availability of the scanner in emergency cases.

The use of the model was applied to real-life data from the Virga Jesse Hospital (Hasselt, Belgium), comparing system performance when using the planned, actual and optimal grouping policy. It has been shown that the use of optimal group sizes leads to a significantly smaller backlog. In addition, the model offers a way to determine the time at which the patient has to be present on the day of the appointment, in order to be sure that the schedule for that day can be met with a certain probability.

REFERENCES

[1] Vandaele N., *'The Impact of Lot Sizing on Queueing Delays: Multi-Product, Multi-Machine Models'*, PhD Thesis, Department of Applied Economics, KULeuven, Leuven, 1996.

[2] Lambrecht M.R., P.L. Ivens, N.J. Vandaele, 'ACLIPS: A Capacity and Lead Time Integrated Procedure for Scheduling', Management Science, 44 (11-1), 1548-1561, 1998.

[3] Truyen L., *'Magnetic resonance imaging studies in multiple sclerosis'*, PhD thesis, Medical Department, Universitaire Instellingen Antwerpen, Antwerp, 1996.

[4] Karmarkar U., '*Lot sizes, lead times and in-process inventories'*, Management Science, 1987, Vol.33, No. 3, p.409 – 423.

[5] Lambrecht M.R., Chen S. and Vandaele N.J.,*'A lot sizing model with queueing delays. The issue of safety time'*, European Journal of Operational Research, 1996, Vol.89, No. 2, p.269-276.

[6] Lambrecht M.R. and Vandaele N.J., *'A general approximation for the single product lot sizing model with queueing delays'*, European Journal of Operational Research, 1996, Vol.95, No.1, p.73-88.

[7] Hopp W. and Spearman M., *'Factory Physics, Foundations of Manufacturing Management'*, Irwin, Chicago, 1996.

[8] Kraemer W.and Lagenbach-Belz M., *'Approximate Formulae for the delay in the queueing system GI/GI/1'*, Congressbook, Eighth International Teletraffic Congress, Melbourne, 1976, p.235-1/8.

[9] Whitt W., *'The queueing network analyzer'*, The Bell System Technical Journal, 1983, Vol.62, No.9, p.2779-2815.